Ecological Informatics 86 (2025) 103043

Contents lists available at ScienceDirect

Ecological Informatics

journal homepage: www.elsevier.com/locate/ecolinf

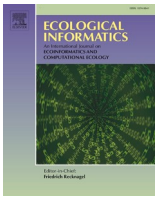

Identifying sources of dissolved organic matter in sediments of a shallow lake by fluorescence and ultraviolet spectral characteristics of water and alkali extractable organic matter (WEOM and AEOM)

Jun Cao [a,b], Tianyu Chen [c,*], Jipeng Sun [d], Jun Zhong [d], Biao Mu [d], Xin Wang [d], Chunyan Wang [a], Massimiliano Materazzi [e], Hualun Zhu [e,*]

[a] National Engineering Research Center of Water Resources Efficient Utilization and Engineering Safety, Hohai University, Nanjing 211111, China
[b] Center for Taihu Basin, Institute of Water Science and Technology, Hohai University, Nanjing 211111, China
[c] Hydraulic Engineering Department, Nanjing Hydraulic Research Institute, Nanjing 210029, China.
[d] College of Environment, Hohai University, Nanjing 211111, China
[e] Department of Chemical Engineering, University College London, London WC1E 7JE, United Kingdom

ARTICLE INFO

Keywords:
Sediments
Dissolved organic matter
Humification index
Fluorescence index
Lake Taihu

ABSTRACT

This study investigates the potential of fluorescence characteristics of dissolved organic matter (DOM) to identify sediment organic matter (OM) sources in shallow lakes. Spectral analyses were performed on water and alkali extractable organic matter (WEOM and AEOM) from Lake Taihu sediments. The lake was divided into seven distinct regions: R1 and R2 strongly influenced by inflowing rivers, R3 and R4 were characterized by submerged macrophytes, and R5-R7 were dominated by cyanobacterial blooms. The investigation illustrated that the highest values of water and alkali extractable organic carbon (WEOC and AEOC) were found in region R4. Specifically, the Humification Index (HIX) values consistently exceeded 2.0 in the northwest regions, contrasting with values predominantly below 1.0 in most southeastern regions. Moreover, the Fluorescence Index (FI) of WEOM in regions R5, R6 and R7 reached 2.10, markedly higher than the values observed in other regions. The horizontal distribution of the four spectrographic indices of AEOM exhibited partial similarity to the distribution pattern of WEOM. Although the WEOC content marginally trailed AEOC, there was a significant correlation between WEOM and AEOM in three indices including slope ratio (S_R), HIX and FI. The identification of sources implied that organic matter in sediments of regions R1 and R2 originated from terrestrial sources, while regions R3 and R4 were largely derived from submerged macrophyte and the regions R5-R7 were notably impacted by cyanobacteria-derived organic matters. Notably, the identification results aligned perfectly with the distribution of inflowing rivers, cyanobacterial blooms and submerged macrophyte coverage within Taihu Lake, underscoring the potential use of dissolved organic matter's spectral characteristics for organic matter source analysis within sediments.

Synopsis: This study identifies distinct sources and spatial distributions of organic matter in Lake Taihu's sediments, using fluorescence characteristics to highlight influences from terrestrial input, submerged macrophytes, and cyanobacterial blooms.

1. Introduction

Dissolved organic matter (DOM) is the most active organic component in soils and water environments, which directly affects the biogeochemical processes and the bioavailability of heavy metals and other pollutants (Chen and Hur, 2015; Feng et al., 2023; Zsolnay, 2003). The inherent complexity and diversity of DOM have been widely recognized (Nebbioso and Piccolo, 2013). Certain components or chemical attributes of DOM can be obtained very easily through straightforward methodologies, such as ultraviolet spectroscopy and fluorescence spectroscopy (Li and Hur, 2017; Pan et al., 2023; Yamashita et al., 2008). In recent years, the spectral and compositional features of DOM have often been used as indices for source identification to infer the source of organic matter and even microbial processes in the

* Corresponding authors.
E-mail addresses: chentianyu8968@outlook.com (T. Chen), hualun-zhu@ucl.ac.uk (H. Zhu).

https://doi.org/10.1016/j.ecoinf.2025.103043
Received 19 July 2024; Received in revised form 20 January 2025; Accepted 20 January 2025
Available online 22 January 2025

environment (Lee et al., 2020; Lin et al., 2023; Oh et al., 2023). Therefore, investigating the spectral and compositional characteristics of DOM in soils and water environments is crucial for understanding the associated biogeochemical processes and tracking its evolution within ecosystems.

Lakes are vital water ecosystems that play a key role in the exchange of essential biological elements, such as carbon and nitrogen, among water, land, and atmosphere. They also provide critical ecological and economic services, including water provisioning, flood mitigation, ecological regulation, storage, landscape enrichment, and resource supply (Heino et al., 2021; Li and Tsigaris, 2024). However, at present, most of the lakes in the world are facing the risk of eutrophication, especially shallow lakes (McCrackin et al., 2017). Compared to deep lakes and reservoirs, sediments in shallow lakes are often disturbed by waves, releasing nutrients that increase eutrophication (Zhou et al., 2022). This process also releases dissolved organic matter (DOM), which in turn influences microbial communities within the water column (Li et al., 2022). Consequently, a comprehensive evaluation of the spectral and compositional characteristics of DOM in shallow lake sediments is urgently needed to assess its impacts on aquatic ecology across different lake regions.

At present, the methods to evaluate the spectral and compositional characteristics of DOM include ultraviolet spectroscopy, Excitation Emission Matrix (EEM) fluorescence combined with Parallel Factor Analysis (PARAFAC), chromatography, nuclear magnetic resonance and Fourier transform ion cyclotron resonance mass spectrometer (FT ICR-MS) (Liu et al., 2023a; Pan et al., 2023; Yamashita et al., 2008). Although mass spectrometry and nuclear magnetic resonance offer comprehensive insights into DOM composition, EEM-PARAFAC stands as the most frequently utilized method. This popularity is owed to its simplicity, cost-effectiveness, and robust capacity for both endogenous and exogenous substance identification (Duan et al., 2022). Ultraviolet spectra are often combined with EEM-PARAFAC to obtain information about the molecular weight and aromaticity of DOM (Kim et al., 2023). In addition, spectral characteristics of DOM were useful for monitoring surface water quality and analyses of the carbon cycle in aquatic ecosystems (Meng et al., 2024). There, the spatial and temporal distribution of spectral and compositional characteristics of DOM in lakes and rivers was still very important to reveal the response of element cycling processes in water ecosystems to environmental changes.

EEM-PARAFAC generally categorizes DOM into two main groups: humic-like and protein-like substances. Humic-like substances are typically derived from the decomposition of terrestrial plant litter in soils and are primarily indicative of terrestrial DOM. In contrast, protein-like substances usually originate from microbial secretions and are commonly used to represent endogenous DOM (Ge et al., 2021; Li et al., 2023). Additionally, specific fluorescence indices, such as the fluorescence index (FI), play a crucial role in source identification, helping to distinguish between terrestrial and microbial DOM (Fellman et al., 2010a). Moreover, FI was used for source identification of organic carbon and nitrate in rivers in recent years (Kim et al., 2023; Lin et al., 2023). The humification index can reflect the degree of microbial degradation of organic matter (Fellman et al., 2010a). Recent studies have increasingly harnessed DOM fluorescence characteristics to identify the sources of organic matter and nitrate in water (Duan et al., 2022; Lin et al., 2023). However, the feasibility of extending this methodology to identify the sources of organic matter in sediments warrants further exploration.

At present, studies of DOM fluorescence spectra in lake sediments primarily focus on the interaction between DOM and nutrient release, microbial community (Li et al., 2022) and pollutants (Fan et al., 2023; Ren et al., 2020) in sediments. Most of these studies collect pore water from sediments, as it is considered to better represent in-situ conditions (Mostofa et al., 2018; Xu et al., 2021). Alternatively, some studies extract organic matter using water or alkali solutions from air-dried or freeze-dried sediments, followed by analysis using fluorescence spectroscopy (Ge et al., 2021; Zhu et al., 2017). This extraction method is particularly suited for larger investigation areas and is more effective for source identification.

Researchers analyzed spectral characteristics of DOM from sediments in Lake Baiyangdian, North China, uncovering EEM-PARAFAC's ability to delineate varying contributions of terrestrial versus autochthonous DOM sources in lake sediments (Yuan et al., 2014). Similar results were reported from the lobelia lakes situated in Pomeranian region (Mielnik and Kowalczuk, 2018). Additional studies indicated that the ratio of humic-like to protein-like substances could serve as an indirect indicator of water quality in the sediments of Dongting Lake and Erhai Lake (Li et al., 2015; Li et al., 2016). This correlation was also evident in eleven New Zealand lakes (Pearson et al., 2022) and Lake Lihu (Wang et al., 2018). In addition, the spectral features of DOM exhibited depth-dependent variations (Song et al., 2019). Collectively, these studies indicated that the fluorescence characteristics of sediment DOM can effectively delineate terrigenous and endogenous sources to a certain extent.

Lake Taihu is a globally recognized lake for studying eutrophication. Spanning hundreds of square kilometers, it experiences recurrent cyanobacterial blooms every summer (Qin et al., 2019). The eastern part of the lake is covered with dense aquatic plants throughout the year (Zhang et al., 2021). Over 20 rivers flow into Lake Taihu from various directions, while only one river drains water from the southeast (Zhang et al., 2017). As a result, the lake's dynamics are influenced by a combination of terrestrial inputs, cyanobacterial sources, aquatic plant-derived material, and other endogenous contributions from microorganisms (Zhang et al., 2018). Particularly, the effects of eutrophication and water blooms on DOM characteristics were received special attentions (Guan et al., 2024). The aim of this study is to investigate the efficacy of utilizing the fluorescence characteristics of DOM to discern sources in this intricate environment. Simultaneously, both horizontal and vertical distributions were studied. Both water and alkali extractable organic matter (WEOM and AEOM) were analyzed to evaluate the similarities and differences in organic matter obtained via different extraction methods. The source identification results obtained in this study will be helpful for understanding the effects of import of terrestrial sources, cyanobacterial blooms occurrence, macro aquatic plant restoration and other processes on the carbon cycle in lake sediments.

2. Materials and methods

2.1. Sediment samples collection

Thirty-eight sampling sites were categorized into seven distinct regions within Lake Taihu for this study (Fig. 1) (Zhang et al., 2017). Region R1 (sites 1–3) is influenced by five rivers and experiences the most severe cyanobacterial blooms during summer, while Region R2 (sites 4–9), characterized by nine flowing rivers, has infrequent blooms. Regions R3 (sites 10–12) and R4 (sites 13–16) are almost entirely covered by dense submerged macrophytes, which limit cyanobacterial blooms (Zhang et al., 2021). Notably, Region R3 serves as the primary outlet of Lake Taihu. Regions R5 (sites 17–21) and R6 (sites 22–26) are two of the lake's three bays most prone to cyanobacterial blooms, with Region R6 additionally influenced by the Yangtze River diversion project, which channels water from the Yangtze River into Lake Taihu. Region R7 (sites 27–38) represents the central part of the lake.

Sample collection was conducted in the autumn of 2023. At each site, sediment cores measuring 20 cm in length were collected using a gravity tube sampler with a 50 cm diameter. Due to variations in sediment depth across the study area, each core was divided into two to four sections at 5 cm intervals. The sediment samples were immediately transported to the laboratory in glass containers for further analysis.

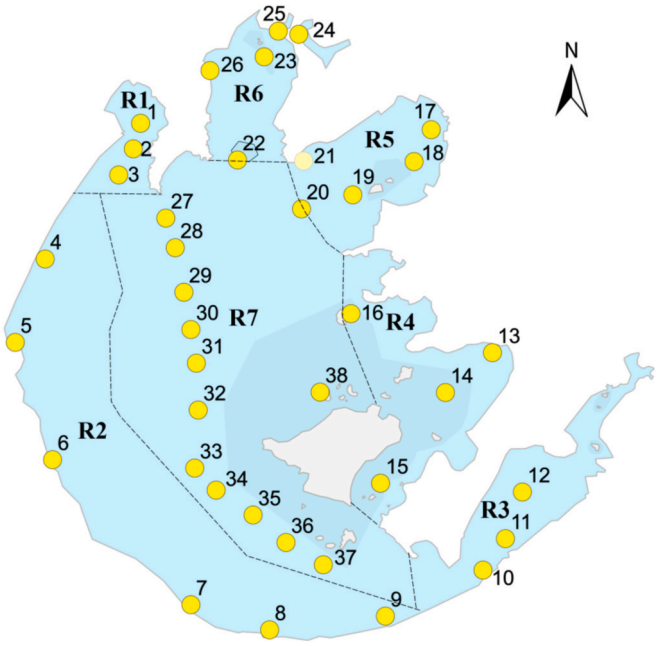

Fig. 1. Sampling sites in various regions (R1-R7) of Lake Taihu.

2.2. Extraction of WEOM and AEOM

All sediment samples were air-dried, ground, and sieved through a 200-mesh sieve to ensure homogenization. The pre-treated samples were then divided into two groups: one group was used to measure the sediment organic carbon (SOC) and total phosphorus (TP) content, while the other group was used for the extraction of WEOM and AEOM.

For the extraction of WEOM, a precisely weighed 3.00 g of pretreated sediment sample was placed into a 50-mL centrifuge tube. Next, 30 mL of deionized water was added, and the tube was shaken in a homothermal water bath oscillator at 60 °C with a rotation speed of 300 rpm for 30 min. The tube was then centrifuged at 10,000 ×*g* for 10 min, and the resulting supernatant was filtered through a 0.45-μm pore-sized membrane. The filtrate was collected as the WEOM sample. AEOM was extracted using the same procedure, except that 0.5 M KOH was used as the extraction solution instead of deionized water.

2.3. Analysis methods

SOC content was analyzed using a total organic carbon analyzer (TOC-L CPN, Shimadzu, Japan) coupled with SSM-5000 A device. The TP content of sediment was analyzed according to the soil sample determination methods outlined in literatures (Bao, 2000). Total phosphorus in the sediments was extracted using hydrochloric and nitric acid and determined by the molybdenum-antimony resistance colorimetry method (Lü et al., 2023).

The dissolved organic carbon (DOC) content in the WEOC and AEOC samples was analyzed using a total organic carbon analyzer (TOC-L CPN, Shimadzu, Japan). The ultraviolet spectra of the WEOM and AEOM samples were measured with a UV–vis spectrometer (UV-1780, Shimadzu, Japan) across a wavelength range of 200 to 400 nm, with a 1-nm step interval. Milli-Q water was used for baseline zero adjustment prior to the analysis.

The fluorescence excitation-emission matrices (EEMs) of the WEOM and AEOM samples were analyzed using a fluorescent spectrometer (RF-6000; Shimadzu). Before the analysis, the DOC content of the WEOC and AEOC samples was diluted to 8 mg/L to avoid the internal filtration effect. Most of the effects concerned with Raman scatter were eliminated by subtracting the Milli-Q blank. The excitation wavelengths ranged from 200 to 500 nm in 10-nm increments, and the emission wavelength ranged from 250 to 550 nm in 2 nm increments. The slit width was set as 5 nm for both excitation and emission and the scan speed was set at 2000 nm/min.

2.4. EEM-PARAFAC and indices calculation

EEM-PARAFAC was performed using the DOM Flour toolbox developed in the previous study (Stedmon and Bro, 2008). To account for internal filter effects in the EEMs, corrections were applied via absorbance spectroscopy, following methods outlined by Fellman et al (Fellman et al., 2010b) PARAFAC modeling was conducted using the DOMFlour toolbox in Matlab 13.0 (MathWorks Inc., USA). Residual and split-half analyses were conducted to determine the correct number of fluorescent components.

The specific UV absorbance ($SUVA_{254}$) and slope ratio (S_R) were calculated using the ultraviolet spectrum. $SUVA_{254}$ was calculated according to Eq. (1) as follows (Zhu et al., 2017).

$$SUVA_{254} = A_{254}/DOC \times 100 \quad (1)$$

Where A_{254} is the UV absorbance at 254 nm, and the DOC represents dissolved organic carbon in the WEOM or AEOM samples.

The slope ratio (S_R) value was calculated based on Eq. (2) (Fellman et al., 2010a):

$$S_R = \sum A_{275-295} \Big/ \sum A_{350-400} \quad (2)$$

Where $\sum A_{275-295}$ is the summation of absorbance values at 275–295 nm, and $\sum A_{350-400}$ is the summation of absorbance values at 350–400 nm.

Two fluorescence indices, HIX and FI, were calculated following Eq. (3) and (4), respectively (Li et al., 2023).

$$HIX = \sum A_{(Em=435-480,Ex=254)} \Big/ \sum A_{(Em=300-445,Ex=254)} \quad (3)$$

Where $\sum A_{(Em=435-480,\ Ex=254)}$ is the summation of emission intensity at 435–480 nm with an excitation wavelength of 254 nm. $\sum A_{(Em=300-445,\ Ex=254)}$ represents the summation of emission intensity at 300–445 nm with an excitation wavelength of 254 nm.

$$FI = A_{450/370}/A_{500/370} \quad (4)$$

Where $A_{450/370}$ is the emission intensity with emission wavelength at 450 nm a with an excitation wavelength of 370 nm. $A_{500/370}$ represents the emission intensity with emission wavelength at 500 nm with an excitation wavelength of 370 nm.

2.5. Data statistics

Given the presence of multiple samples in each region, none of the tests in this study were conducted in parallel. However, for every 8–10 samples analyzed, we placed a quality control sample with a known concentration to ensure the accuracy of the test. The relative standard deviation of DOC analysis was 4.15 %. The significant differences among various regions were determined by analysis of variance (ANOVA) using a Tukey post hoc test via SPSS 16.0. Spearman correlation among various indices were carried out using R Studio (Server V 1.4.1717) with corrplot packages.

3. Results

3.1. Organic carbon and total phosphorus in sediments

The SOC content ranged from 14 to 52 g/kg, with a significantly higher average value observed in region R1 compared to other regions (Fig. 2a). In contrast, the WEOC content ranged from 0.13 to 1.10 g/kg, while AEOC values were slightly higher (Fig. 2b). The highest average values for both WEOC and AEOC were recorded in region R4. The TP

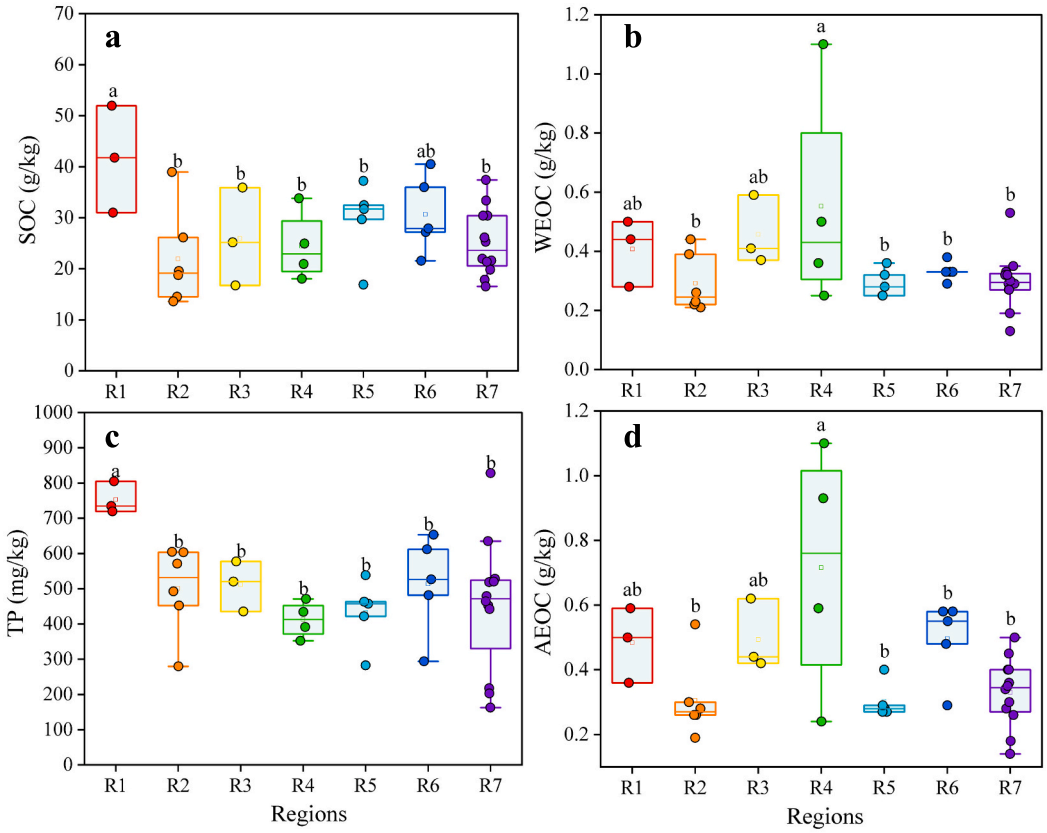

Fig. 2. The content of SOC (a), WEOC (b), TP (c) and AEOC (d) of sediments in various regions. Different lowercase letters above each boxplot indicate significant differences ($P < 0.05$) among samples in various regions.

content varied between 162 and 828 mg/kg, with region R1 showing a significantly higher average value than the other regions (Fig. 2d).

3.2. Horizontal distribution of EEM components and spectral indices

Three fluorescence components were identified using EEM-PARAFAC (Fig. 3). The first component, C1, exhibited two peaks ($\lambda_{Ex/Em}$ = 230/400 nm and $\lambda_{Ex/Em}$ = 310/400 nm) and was identified as an Ultraviolet A (UVA) humic-like component (Fellman et al., 2010a). This component is commonly found in wastewater, wetlands, and agricultural environments and is associated with biologically active organic matter of low molecular weight. The second component, C2, also displayed two peaks ($\lambda_{Ex/Em}$ = 220/290 nm and $\lambda_{Ex/Em}$ = 275/290 nm) and was identified as a protein-like component (Santín et al., 2009), likely derived from microbial secretions (Ge et al., 2021; Guo et al., 2022). Similar peaks have been observed in the extracellular polymeric substances (EPS) of green algae (Liu et al., 2023a). The third component, C3, showed a maximum intensity at an excitation wavelength of 260 nm and an emission wavelength of 460 nm. This component was classified as a UVC humic-like component (Fellman et al., 2010a) with high molecular weight and is commonly found in soils (Pan et al., 2023).

The proportion of the UVA humic-like component C1 in WEOM ranged from 20 % to 30 % in most cases, showing no significant differences among the regions (Fig. 3d). In contrast, the proportion of the UVC humic-like component C3 remained below 25 % across all regions, with region R4 exhibiting a notably lower proportion compared to other regions. However, the protein-like component C2 accounted for average values above 50 % in nearly all regions. Notably, the proportion of C2 in region R1 was significantly lower than in the other regions.

The distribution of fluorescence components in AEOM showed noticeable differences compared to WEOM. Specifically, the proportion of C1 in AEOM displayed minimal variation across the regions, with no significant differences observed. In contrast, the average proportion of the protein-like component C2 in AEOM was highest in region R7 and lowest in region R3. Interestingly, the distribution pattern of the UVC humic-like component C3 in AEOM across the regions was nearly the opposite of that observed for C2.

Fig. 4 illustrates that the highest $SUVA_{254}$ value (1.68) of WEOM was found in region R2 and the northern part of region R6. S_R of WEOM ranged from 3.12 to 10.8, with significantly higher values recorded in region R7 compared to other regions. Moreover, the HIX values in the northwest regions consistently surpassed 2.0, in contrast to values below 1.0 in most southeastern regions. For the FI of WEOM, regions R5, R6 and R7 exhibited values reaching up to 2.10, which were markedly higher than those in other regions. The horizontal distribution patterns of the four spectrographic indices of AEOM showed similarities to those of WEOM. However, the values of $SUVA_{254}$ and HIX for AEOM were much higher than those for AEOM.

3.3. Vertical distribution of EEM components and spectral indices

The verticle distribution of SOC, WDOC, TP and AEOC is depicted in Fig. 5. The first three indicators decreased with increasing sediment depth, while the AEOC demonstrated an increase. The maximum SOC value (89 g/kg) was observed at the surface layer, while the lowest value (10 g/kg) was found at the bottom. The TP content in the bottom sediments ranged from 298 to 525 mg/kg. The average value of WDOC decreased from 0.34 g/kg in the surface layer to 0.23 g/kg at the bottom. In contrast, the average AEOC content increased progressively from 0.41 g/kg to 0.52 g/kg, 0.57 g/kg, and 0.67 g/kg from the surface to the bottom layers, respectively.

For WEOM, $SUVA_{254}$ and FI exhibited a decreasing trend with increasing sediment depth (Fig. 6). The average values of $SUVA_{254}$ and FI of WEOM in the surface sediments were 0.77 and 1.77 but the values

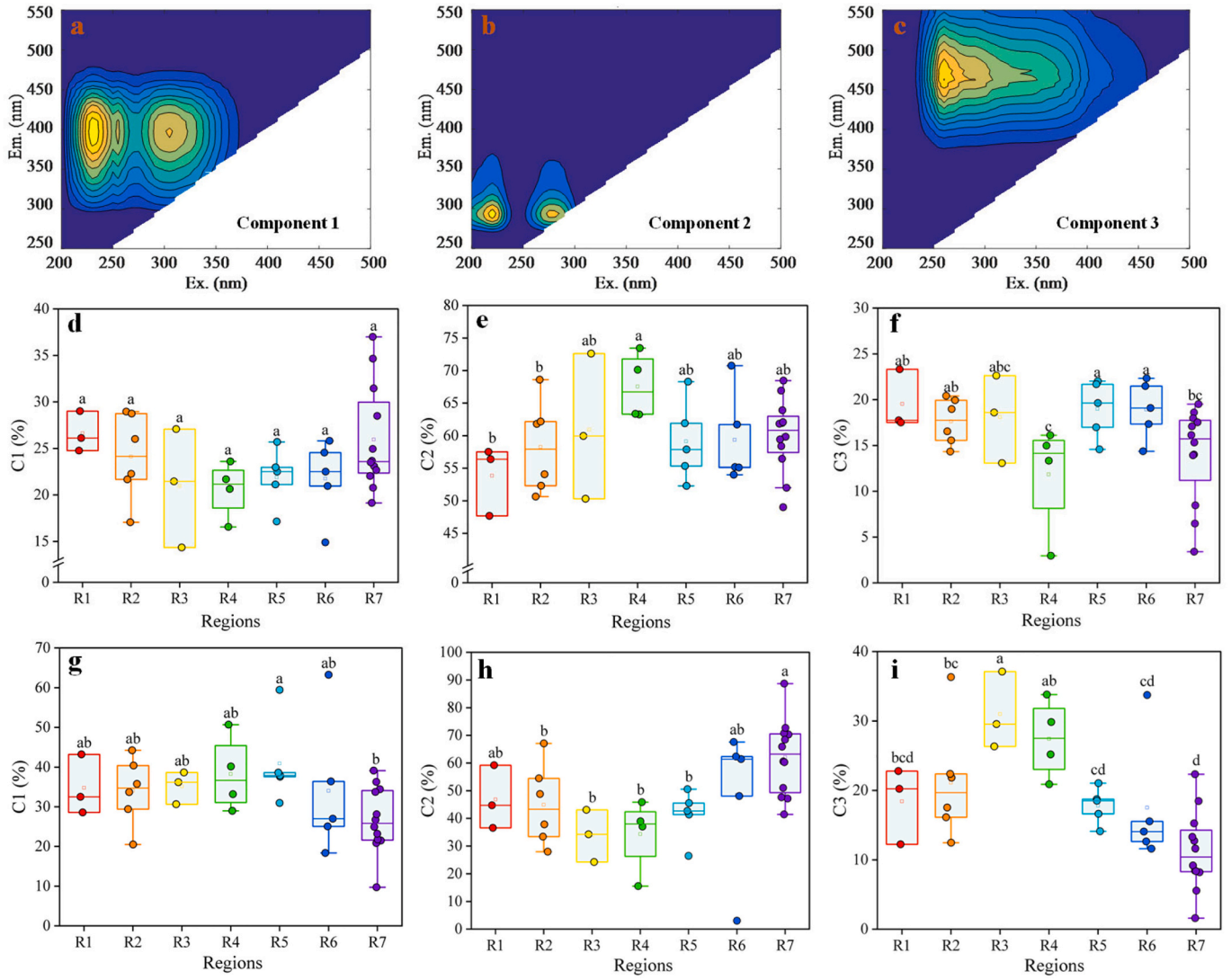

Fig. 3. EEM-PARAFAC components and the proportion of C1-C3. a-c: for the EEMs; d-f: for the fraction of each component in WEOM; d-f: for the fraction of each component in AEOM. Different lowercase letters above each boxplot indicate significant differences ($P < 0.05$) among samples in various regions.

in the bottom sediments were 0.52 and 1.70, respectively. S_R The S_R values showed no significant differences across the top three layers; however, they were significantly higher than those observed in the bottom layer. Notably, the lowest average value of HIX was found in the second top layer.

In AEOM, both S_R and FI decreased with increasing sediment depths (Fig. 7). The average values of S_R and FI at the surface sediments were 4.70 and 1.76 respectively, while these values decreased to 3.66 and 1.65 in the bottom sediments. The HIX values in the top two layers were significantly lower than those in the bottom two layers. There was no obvious vertical variation observed in $SUVA_{254}$ of AEOM. In addition, the vertical distribution of the proportions of EEM components in both WEOM and AEOM did not show any obvious trends (Fig. 8).

3.4. Correlation among SOC and TP content and spectral indices in WEOM and AEOM

The SOC content exhibited a significant positive correlation with TP content (Fig. 9a, b). Furthermore, the TP content was significantly and positively related to HIX and the proportion of C3 in WEOM, while showing negative correlations with spectral SR and the proportion of C2 in WEOM. However, no significant correlations were observed between TP content and spectral indices in either WEOM or in AEOM. Notably, a positive relationship between HIX and $SUVA_{254}$ was noted in both WEOM and AEOM. Conversely, a significant negative correlation was found between S_R and FI in both WEOM and AEOM.

The relationship among spectral indices between WEOM and AEOM was analyzed using Spearman correlation. The results showed that there were significant correlations between WEOM and AEOM in three indices including S_R, HIX and FI (Fig. 9c). However, there were few significant correlations between WEOM and AEOM for the EEM components.

4. Discussion

4.1. Source identification based on horizontal distribution of spectral characteristics of WEOM and AEOM

Our findings revealed that the SOC and TP contents in R1 region were significantly higher than those in other regions (Fig. 2). However, both WEOC and AEOC reached their maximum levels in region R4. Although this data alone was insufficient to fully infer the sources and dynamics of organic matter in Lake Taihu's sediments, the distinct horizontal distribution patterns of WEOM and AEOM offered valuable insights into the sources and dynamics of organic matter.

Although WEOC and AEOC exhibited notable differences, their SR, HIX, and FI values showed clear consistency in horizontal distribution.

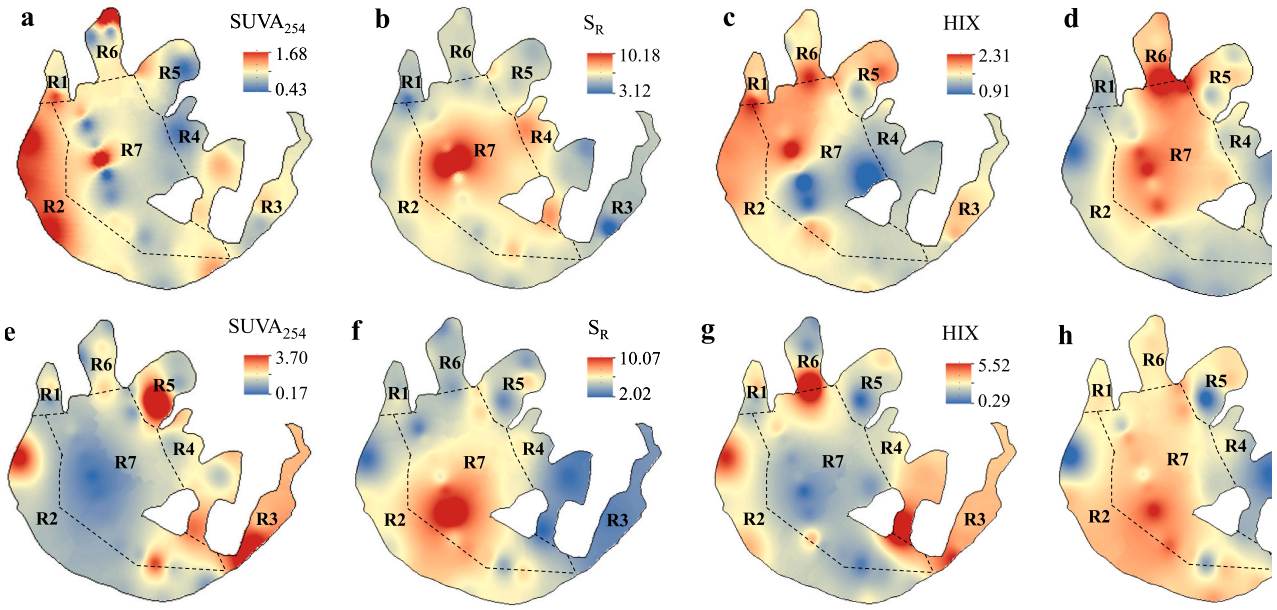

Fig. 4. Horizontal distribution of the indices of ultraviolet and fluorescence spectra of WEOM (a-d) and AEOM (e-h) in the surface sediments.

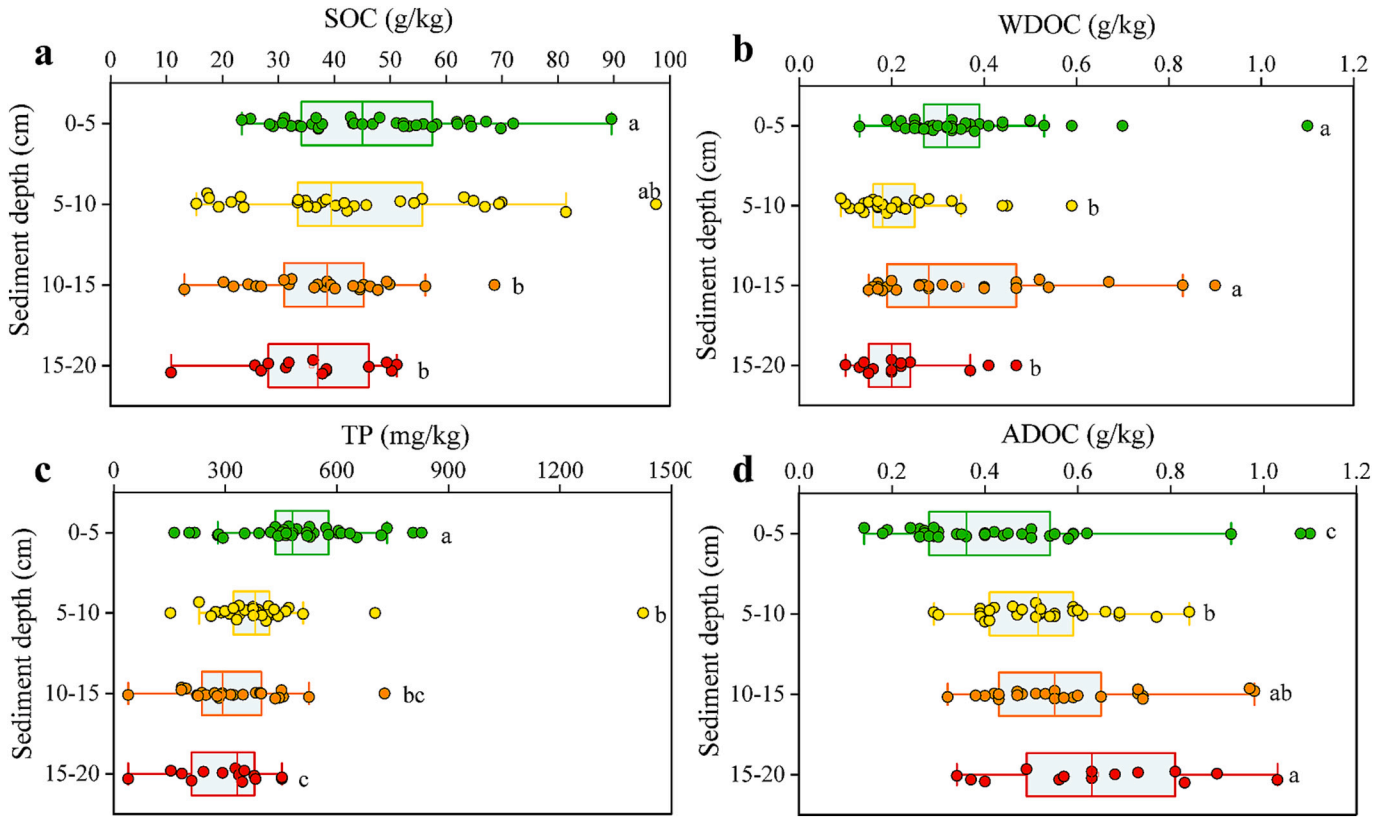

Fig. 5. The verticle distribution of SOC (a), WDOC (b), TP (c) and AEOC (d). Different lowercase letters to the right of each boxplot indicate significant differences ($P < 0.05$) among samples in various depths.

These indices demonstrated significant positive correlations between WEOM and AEOM, suggesting that the fluorescence indices of both can be effectively used to infer the sources of extractable organic matter in sediments. To enhance this inference, the fluorescence indices of WEOM were specifically utilized as indicators for identifying the sources of extractable organic matter in sediments. Therefore, the scatter plots of FI and HIX of WEOM and AEOM in the surface sediments were established as Fig. 10 to clearly illustrate the sources of DOM in sediments.

The FI is one of the most commonly used indices for sources identification (Fellman et al., 2010a; Lin et al., 2023). Typically, the FI value for terrestrial DOM ranges between 1.6 and 1.7, whereas endogenous DOM, such as microbial secretions, can have values exceeding 2.1 (Wen et al., 2023). I n this study, the FI values in regions R1–R4 were significantly lower than those in regions R5–R7. Specifically, regions R1 and

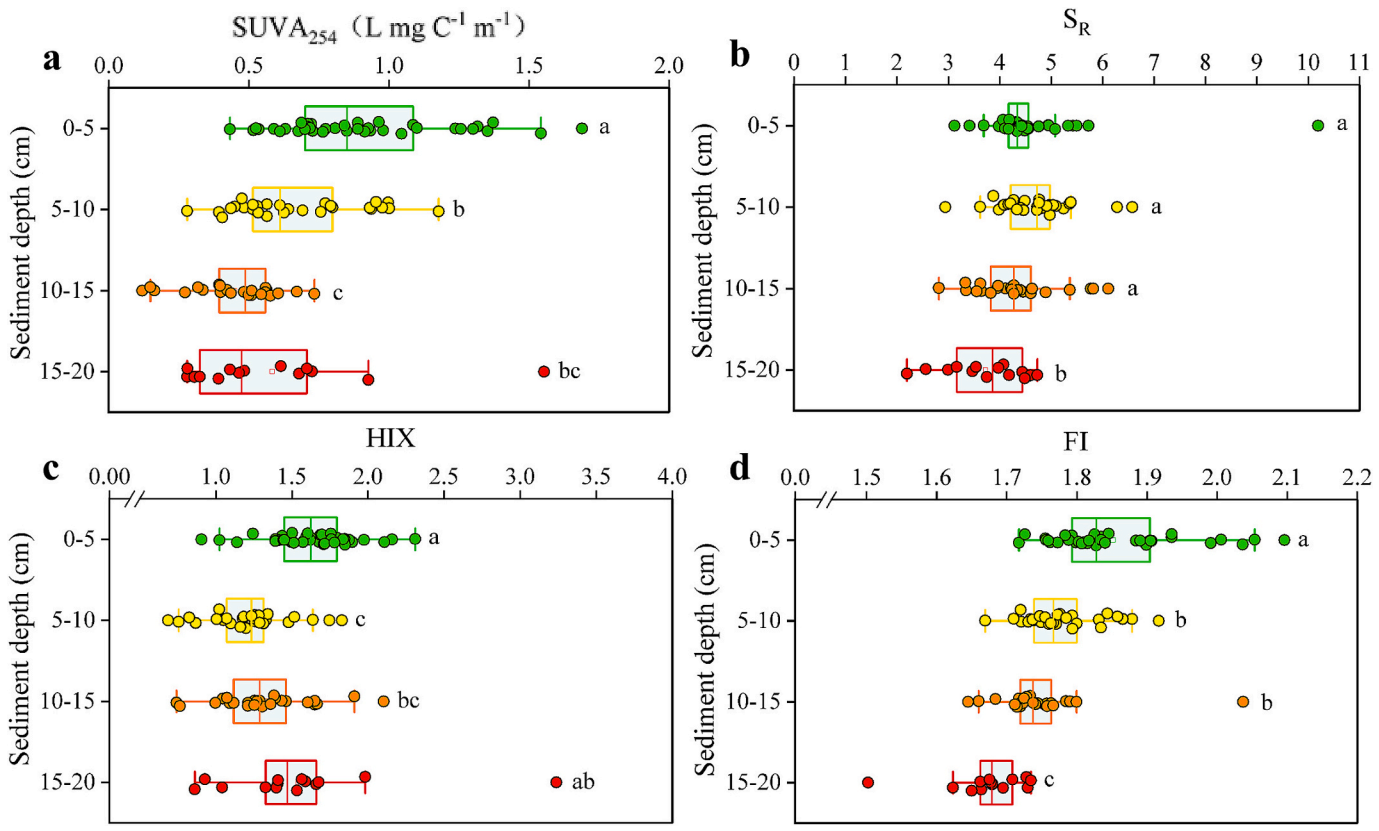

Fig. 6. Vertical distribution of the indices of ultraviolet and fluorescence spectra of WEOM. Different lowercase letters to the right of each boxplot indicate significant differences ($P < 0.05$) among samples in various depths.

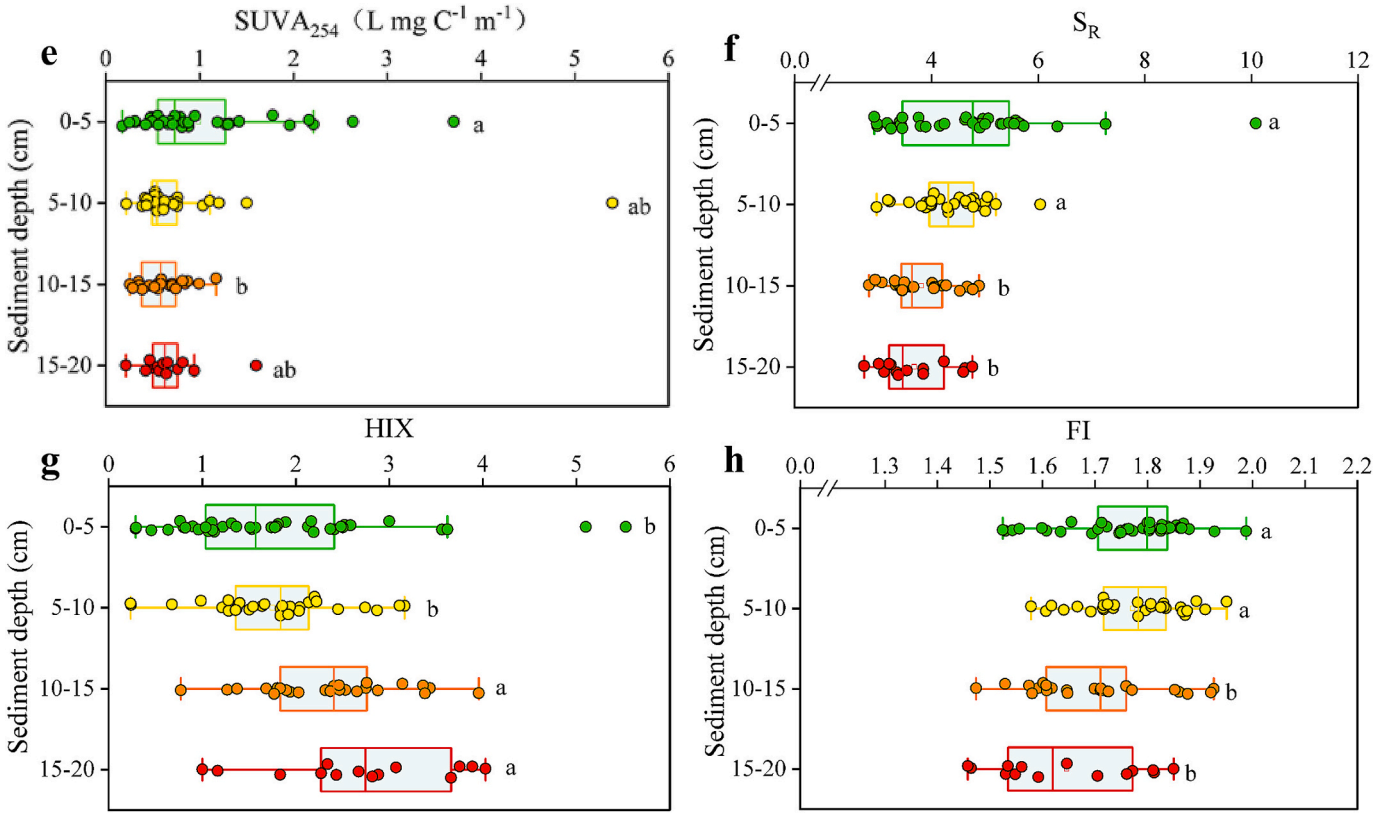

Fig. 7. Vertical distribution of the indices of ultraviolet and fluorescence spectra of AEOM. Different lowercase letters to the right of each boxplot indicate significant differences ($P < 0.05$) among samples in various depths.

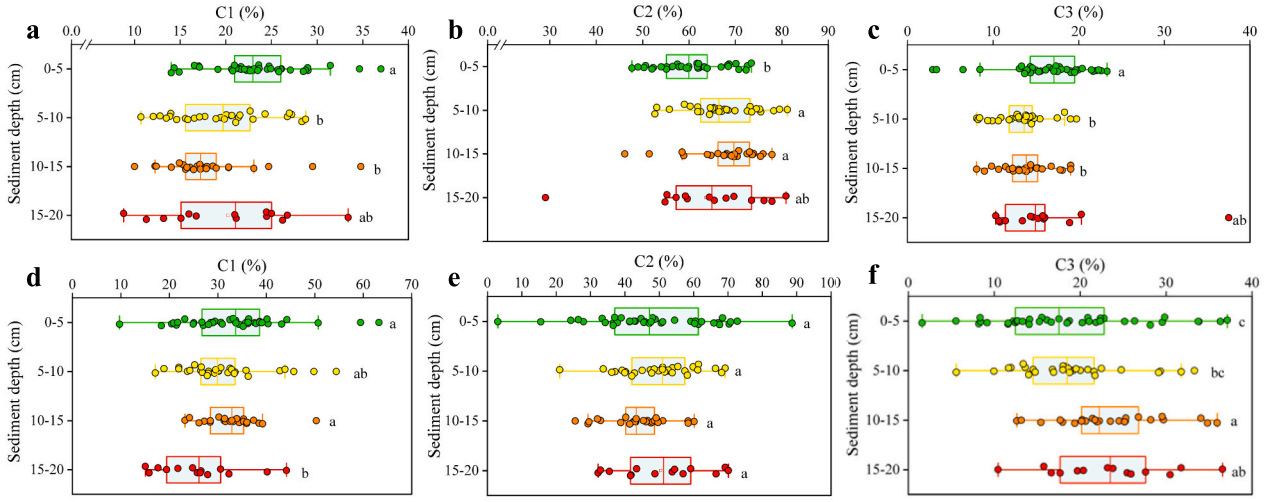

Fig. 8. The propotion of EEM-PARAFAC components C1-C3 of WEOM and AEOM of sediments in various depths. Different lowercase letters to the right of each boxplot indicate significant differences ($P < 0.05$) among samples in various depths.

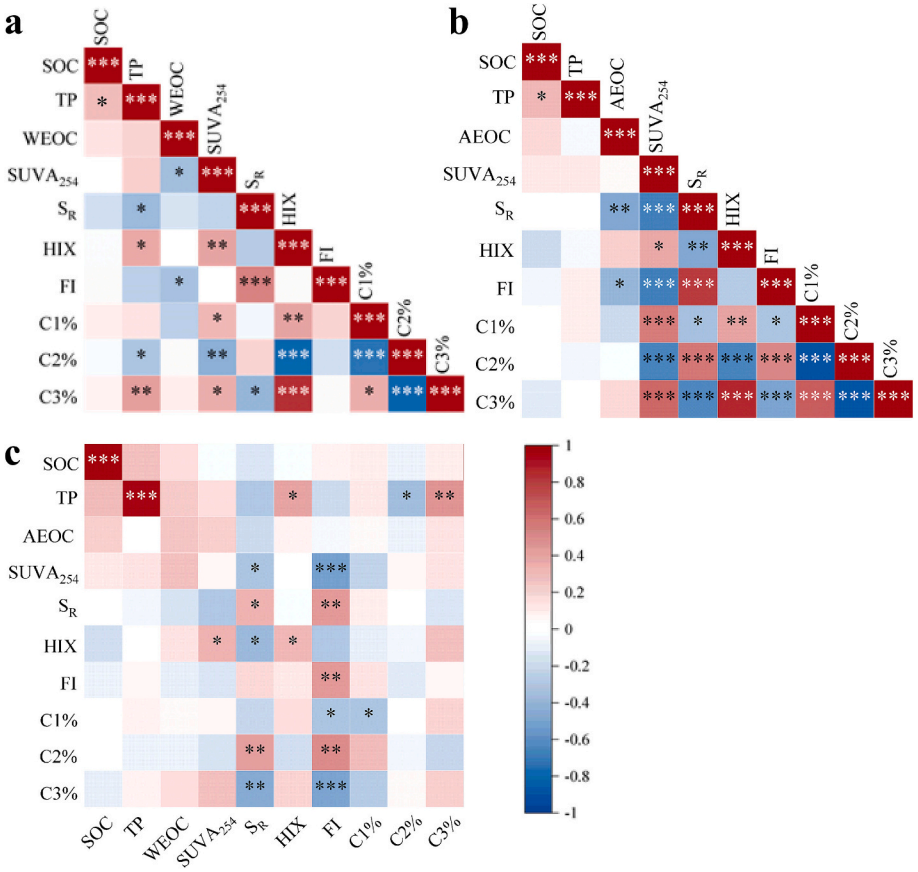

Fig. 9. Spearman correlation among SOC and TP content and spectral indices in WEOM (a), AEOM (b) and correlation of each index between WEOM and AEOM (c). *: $p \leq 0.05$; **: $p \leq 0.01$; ***: $p \leq 0.001$.

R2, influenced by multiple river inflows, contain abundant terrestrial organic matter. Conversely, regions R3 and R4, which host extensive aquatic plant populations, contribute organic matter with characteristics similar to terrestrial sources (Dong et al., 2014). The FI value of WEOC in regions R1–R4 was approximately 1.7, indicating a dominance of terrestrial DOM. These findings suggest that WEOM in regions R1 and R2 primarily originates from terrestrial DOM inputs via rivers, while WEOM in regions R3 and R4 is mainly derived from aquatic plants (Zhang et al., 2017). This deduction aligns with the scatter plots of FI and HIX for WEOM shown in Fig. 10.

In contrast, regions R5–R7 had minimal aquatic plant growth and were fed by only a few rivers (Dong et al., 2014). However, severe cyanobacterial blooms frequently occurred in regions R5 and R6, as well as in the northwest of region R7 (Yang et al., 2016; Zhu et al., 2014). Researchers analyzed the EPS characteristics of cyanobacteria, green algae and diatoms (five species each), and found that the FI values of

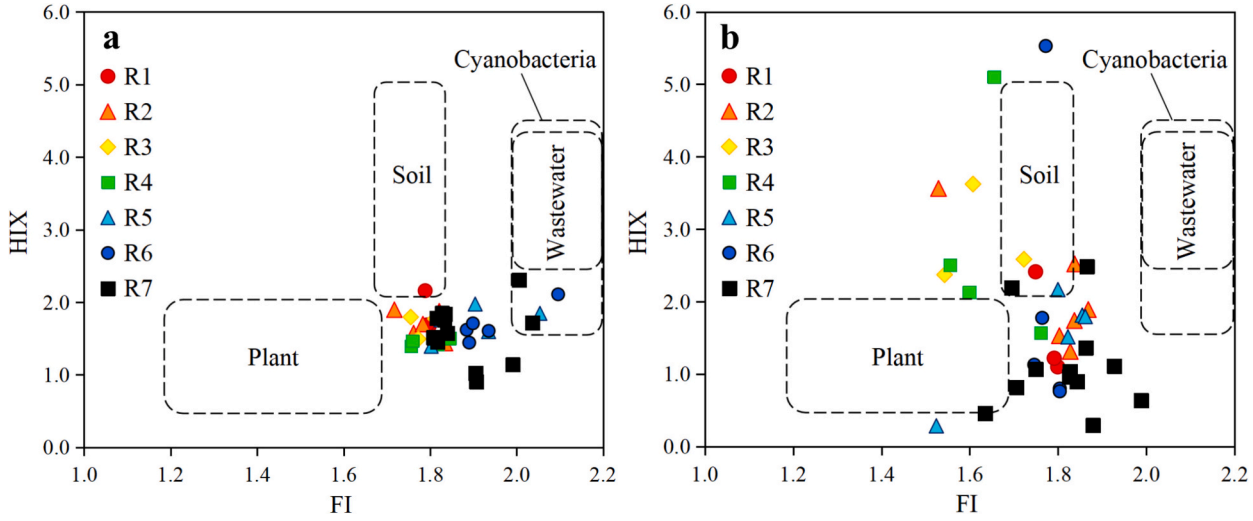

Fig. 10. Scatter plots of FI and HIX of WEOM (a) and AEOM (b) in the surface sediments. Indices from different sources were located according to previous studies. (Hunt and Ohno, 2007; Kim et al., 2023; Liu et al., 2023b; Wen et al., 2023; Zhou et al., 2021; Zhuang et al., 2021)

cyanobacteria mostly exceeded 2.1, while the FI values of eukaryotic microalgae such as green algae and diatoms remained below 1.7 (Liu et al., 2023a). In this study, the FI value of WEOM in the sediments from these regions was approximately 2.0 (Fig. 10), closely aligning with the FI values of cyanobacterial EPS. Furthermore, Fig. 10 illustrated that some sites in regions R5, R6, and R7 fell within the cyanobacteria range, a result consistent with previous analyses using lipid biomarkers (Zhang et al., 2017). These findings suggest that WEOM in the sediments from these areas likely originates in part from cyanobacteria-derived DOM.

HIX reflected the degree of degradation of DOM (Fellman et al., 2010a). While there are significant differences in the HIX values of DOM from various sources, HIX primarily indicates the residual DOM after microbial degradation (Li et al., 2023). In this study, the HIX value of WEOC was generally higher in the northwest area of Lake Taihu. This observation aligns with the prevailing southeast winds during summer and autumn, which transport large amounts of cyanobacterial scum toward the northwest lake area. Research indicates that the HIX value for cyanobacteria ranges from 1.7 to 5.4, whereas values for green algae and diatoms remain below 1.3 (Liu et al., 2023b). In comparison, the HIX of soil DOM typically falls between 2 and 5, while plant leaf-derived DOM ranges from 0.5 to 2.0. Considering the FI values in regions R1 and R2 (Fig. 10), it is evident that terrestrial sources dominate these areas, contrasting with the greater cyanobacteria-derived contributions in regions R5, R6, and R7. Therefore, it can be concluded that regions R5, R6 and R7 mainly derive their organic matter from cyanobacteria. Interestingly, despite the dominance of cyanobacterial blooms in region R1, river inflows may impede the accumulation of cyanobacteria-derived organic matter in this region.

The protein-like fluorescent component C2 showed the highest prevalence in region R4, while it had the lowest occurrence in region R1. Conversely, the UVC humic-like component C3 displayed its lowest representation in region R4. These results indicated that there was more input of fresh organic matter in R4 region, while the proportion of fresh organic matter in R1 region was the least. This observation aligns with earlier inferences that terrestrial sources contributed more significantly to region R1, whereas aquatic plants played a more prominent role in region R4. These findings are consistent with previous studies, which suggest that aquatic macrophytes can reduce sediment resuspension and, consequently, limit OM degradation (Zhang et al., 2021). In addition, a previous study showed that the porportion of a UVC humic-like component in the extracellular polymer of the bloom-forming cayno-bacterium *Microcystis* was larger than 40 % (Xiao et al., 2019). The fluorescence peak of this UVC humic-like component was similar to the component C3 in the current study. The porportion of component C3 in regions of R5 and R6 influenced by cyanobacterial blomms was also higher than the value in the regions covered by dense submerged macrophytes (R3 and R4). Guan et al. (2024) also found that this UVC humic-like component C3 was the primary component in plateau lakes and the proportion of this component increased with the increasing eutrophication levels (Guan et al., 2024). All the above results indicated that the DOM in the sediment still retained some characteristics of the DOM sources.

$SUVA_{254}$ represented the aromaticity index of DOM (Li et al., 2023). Notably, only region R6 and the northern part of region R1 had a significantly higher HIX value than the other regions. Researchers concluded in the latest study that $SUVA_{254}$ is significantly negatively correlated with FI and positively correlated with HIX (Li et al., 2023). As shown in Fig. 4, the horizontal distribution patterns of $SUVA_{254}$, FI, and HIX aligned with the expected correlations, where $SUVA_{254}$ was negatively correlated with FI and positively correlated with HIX. Additionally, S_R was typically negatively correlated with molecular weight, making it a useful semi-quantitative indicator for assessing molecular weight (Fellman et al., 2010a). In this study, the molecular weight of WEOM in the central lake region (R7) was generally small, while the molecular weight of WEOM in the coastal regions was relatively large. This trend likely resulted from distinct sources: terrestrial input in the western coastal zone, cyanobacterial influences in the northern area, and contributions from aquatic plants in the eastern coastal region. These sources are associated with relatively higher molecular weights of organic matter. On the contrary, WEOC in the central region of the lake might stem from endogenous sources, such as microorganisms and some eukaryotic algae, which typically produce lower-molecular-weight organic matter.

In addition to DOM sources, environmental factors such as wind direction, seasonal variations, and anthropogenic activities significantly impact the fluorescence indices FI, HIX, and SR, further contributing to spatial and temporal DOM variability (He et al., 2022). For example, wind-driven mixing can spread organic matter across different lake regions, bringing more terrestrially derived material into affected areas, which then impacts the fluorescence signals. Seasonal temperature fluctuations play a role as well; warmer months can enhance microbial decomposition and humification processes, raising HIX values (Lee et al., 2019). Rainfall and runoff, more prevalent in certain seasons, introduce terrestrial organic matter, impacting FI and SR indices by altering the organic input sources. Additionally, anthropogenic activities, such as agricultural runoff and wastewater discharge, increase

nutrient loading, which promotes algal blooms and augments autochthonous DOM production, further influencing FI and HIX values (Lan et al., 2024). These findings underscore the complex interplay between environmental factors and DOM sources, providing a more comprehensive perspective on DOM dynamics in Lake Taihu.

4.2. Vertical distribution and correlation among various spectral indices in WEOM and AEOM

Sediments in shallow lakes like Lake Taihu are typically believed to be constantly suspended and redeposited due to winds and waves. However, this study identified a notable trend: SOC and TP contents in the sediment of Lake Taihu exhibited a significant decreasing tendency with depth, indicating that the deep sediments are less disturbed. While the vertical distribution of WEOC was not pronounced, the FI value of WEOC decreased significantly with depth, a pattern also observed in the vertical variation of the FI value of AEOM. This phenomenon suggests that terrestrial sources contributed more to the bottom WEOM, while cyanobacterial and other microbial sources were more prevalent in surface sediments. This may be attributed to the greater resistance of terrestrial organic matter to degradation, allowing it to be better preserved in deeper sediment layers (Fitch et al., 2018). These findings strongly indicate the presence of relatively stable sediment layers within Lake Taihu.

The HIX value of AEOM increased significantly with the increase of depth, while the S_R value decreased, indicating that less fresh organic matter input was obtained by the bottom sediment. This trend reflects a decomposition process, where smaller, easily degradable organic molecules in the bottom AEOM have already broken down, leaving larger molecular-weight organic matter preserved, which contributes to the observed decrease in S_R. However, the vertical distribution of the three fluorescent components in both WEOM and AEOM did not exhibit distinct patterns in this study.

There was no significant correlation between SOC and the other indices. However, TP content demonstrated a significant positive correlation with the HIX of WEOM and a significant negative correlation with S_R. The high HIX value of WEOM in Lake Taihu sediments was primarily associated with DOM from terrestrial and cyanobacterial sources. In this study, only region R1 exhibited significantly higher TP content compared to other regions, coinciding with substantial river inflows. This suggests that the spatial distribution of total phosphorus in the sediments of Lake Taihu is likely influenced by the contribution of terrestrial sources.

While prior studies often revealed a significant positive correlation between DOC and SOC in soils (Zhang et al., 2019a; Zhang et al., 2019b), our study presents an intriguing contrast. We found no significant correlation between WEOC/AEOC and SOC content. Instead, a noteworthy negative correlation emerged between both WEOC and AEOC and the FI. This phenomenon indicated that the abundance of WEOC and AEOC did not depend on SOC, but on the nature of organic matter contributions. A low FI typically indicated the presence of terrestrial organic matter. In this study, only regions R4 and R3 with the highest and second highest WEOC and AEOC, exhibited the densest distribution of aquatic plants in Lake Taihu. The dense aquatic plants in these regions increased the content of EOM in the sediments. This could elucidate why regions R4 and R3, characterized by dense aquatic plant cover, displayed the highest and second-highest average values of both WEOC and AEOC, respectively.

In both WEOM and AEOM, FI exhibited a significant positive correlation with S_R. This implied that the molecular weight of the terrestrial DOM was larger, while the molecular weight of the cyanobacterial and microbial DOM was smaller. In this study, humic acids-like components C1 and C3 were significantly positively correlated with each other, while both were significantly negatively correlated with the protein-like component C2. In addition, C1 and C3 were significantly positively correlated with HIX, and C2 was significantly negatively correlated with HIX. These relationships showed that HIX reflected the presence of abundant humic acids. Furthermore, the significant positive correlation between HIX and $SUVA_{254}$ underscores the alignment between HIX and the aromaticity index, indicating that both indices effectively represent the molecular complexity of DOM.

Although the sources of DOM in sediments of Lake Taihu were revealed to a large extent, the contribution of these sources had not been quantitatively calculated in this study. This limitation was caused by the fact that the source identification algorithm using DOM fluorescence features was not advanced enough. Therefore, a breakthrough in the algorithm is needed in the subsequent research. In addition, the degradation process of DOM in sediments by microorganisms had not been fully considered. This limitation led to uncertainty in the source identification in the current study. This uncertainty can only be identified gradually after further research on the relationship between DOM fluorescence characteristics and microbial activity and community composition.

5. Conclusion

This study provides a comprehensive analysis of the spatial distribution of DOM in Lake Taihu's sediments, highlighting distinct sources across different regions. The findings reveal that regions R1 and R2, influenced by river inflows, are dominated by terrestrial organic matter, while regions R3 and R4, influenced by macrophytes, and regions R5 to R7, affected by cyanobacterial blooms, display unique organic matter profiles. The highest concentrations of WEOC and AEOC were observed in R4, while FI values were elevated in cyanobacteria-dominated areas, indicating the influence of cyanobacterial activity on organic matter composition.

These results have significant implications for lake management and restoration efforts. The study highlights the effectiveness of WEOM over AEOM in identifying sediment sources, which can be used to guide strategies for mitigating nutrient loading, improving water quality, and controlling cyanobacterial blooms. By understanding the distinct horizontal and vertical distributions of DOM, this research provides valuable insights that can support targeted interventions to restore lake health and enhance ecosystem resilience.

CRediT authorship contribution statement

Jun Cao: Writing – original draft, Investigation, Data curation, Conceptualization. **Tianyu Chen:** Writing – review & editing. **Jipeng Sun:** Investigation, Data curation. **Jun Zhong:** Investigation, Data curation. **Biao Mu:** Investigation, Data curation. **Xin Wang:** Investigation, Data curation. **Chunyan Wang:** Writing – review & editing. **Massimiliano Materazzi:** Writing – review & editing. **Hualun Zhu:** Writing – review & editing, Resources.

Acknowledgements

This work was supported by National Natural Science Foundation of China (No. 52076067), National Key Research and Development Program of China (No. 2022YFC3202705).

Appendix A. Supplementary data

Supplementary data to this article can be found online at https://doi.org/10.1016/j.ecoinf.2025.103043.

Data availability

All data used to create the figures are openly provided in the Supplementary Material.

References

Bao, S., 2000. Soil and Agricultural Chemistry Analysis. China agriculture press, Beijing.

Chen, M., Hur, J., 2015. Pre-treatments, characteristics, and biogeochemical dynamics of dissolved organic matter in sediments: a review. Water Res. 79, 10–25.

Dong, B., Qin, B., Gao, G., Cai, X., 2014. Submerged macrophyte communities and the controlling factors in large, shallow Lake Taihu (China): sediment distribution and water depth. J. Great Lakes Res. 40 (3), 646–655.

Duan, P., Wei, M., Yao, L., Li, M., 2022. Relationship between non-point source pollution and fluorescence fingerprint of riverine dissolved organic matter is season dependent. Sci. Total Environ. 823, 153617.

Fan, T., Yao, X., Sun, Z., Sang, D., Liu, L., Deng, H., Zhang, Y., 2023. Properties and metal binding behaviors of sediment dissolved organic matter (SDOM) in lakes with different trophic states along the Yangtze River basin: a comparison and summary. Water Res. 231, 119605.

Fellman, J.B., Hood, E., Spencer, R.G., 2010a. Fluorescence spectroscopy opens new windows into dissolved organic matter dynamics in freshwater ecosystems: a review. Limnol. Oceanogr. 55 (6), 2452–2462.

Fellman, J.B., Spencer, R.G.M., Hernes, P.J., Edwards, R.T., D'Amore, D.V., Hood, E., 2010b. The impact of glacier runoff on the biodegradability and biochemical composition of terrigenous dissolved organic matter in near-shore marine ecosystems. Mar. Chem. 121 (1), 112–122.

Feng, G., Liu, J., Li, H., Liu, J.-S., Duan, Z., Wu, L., Gao, Y., Meng, X.-Z., 2023. Insights from colony formation: the necessity to consider morphotype when assessing the effect of antibiotics on cyanobacteria. Water Res. 246, 120704.

Fitch, A., Orland, C., Willer, D., Emilson, E.J.S., Tanentzap, A.J., 2018. Feasting on terrestrial organic matter: dining in a dark lake changes microbial decomposition. Glob. Chang. Biol. 24 (11), 5110–5122.

Ge, Z., Gao, L., Ma, N., Hu, E., Li, M., 2021. Variation in the content and fluorescent composition of dissolved organic matter in soil water during rainfall-induced wetting and extract of dried soil. Sci. Total Environ. 791, 148296.

Guan, Y., Yu, G., Jia, N., Han, R., Huo, D., 2024. Spectral characteristics of dissolved organic matter in Plateau Lakes: identifying eutrophication indicators in Southwest China. Eco. Inform. 82, 102703.

Guo, L., Xing, A., Zhu, W., Li, F., Guo, Z., 2022. Enhanced methanol-to-olefins (MTO) performance over SAPO-34 molecular sieves synthesized using novel sources of silicon and aluminium. Clean Energy 6 (3), 528–533.

He, J., Wu, X., Zhi, G., Yang, Y., Wu, L., Zhang, Y., Zheng, B., Qadeer, A., Zheng, J., Deng, W., 2022. Fluorescence characteristics of DOM and its influence on water quality of rivers and lakes in the Dianchi Lake basin. Ecol. Indic. 142, 109088.

Heino, J., Alahuhta, J., Bini, L.M., Cai, Y., Heiskanen, A.S., Hellsten, S., Kortelainen, P., Kotamäki, N., Tolonen, K.T., Vihervaara, P., 2021. Lakes in the era of global change: moving beyond single-lake thinking in maintaining biodiversity and ecosystem services. Biol. Rev. 96 (1), 89–106.

Hunt, J.F., Ohno, T., 2007. Characterization of fresh and decomposed dissolved organic matter using excitation− emission matrix fluorescence spectroscopy and multiway analysis. J. Agric. Food Chem. 55 (6), 2121–2128.

Kim, M.-S., Lim, B.R., Jeon, P., Hong, S., Jeon, D., Park, S.Y., Hong, S., Yoo, E.J., Kim, H. S., Shin, S., 2023. Innovative approach to reveal source contribution of dissolved organic matter in a complex river watershed using end-member mixing analysis based on spectroscopic proxies and multi-isotopes. Water Res. 230, 119470.

Lan, J., Liu, P., Hu, X., Zhu, S., 2024. Harmful algal blooms in eutrophic marine environments: causes, monitoring, and treatment. Water 16 (17), 2525.

Lee, Y.K., Lee, M.-H., Hur, J., 2019. A new molecular weight (MW) descriptor of dissolved organic matter to represent the MW-dependent distribution of aromatic condensation: insights from biodegradation and pyrene binding experiments. Sci. Total Environ. 660, 169–176.

Lee, M.-H., Lee, S.Y., Yoo, H.-Y., Shin, K.-H., Hur, J., 2020. Comparing optical versus chromatographic descriptors of dissolved organic matter (DOM) for tracking the non-point sources in rural watersheds. Ecol. Indic. 117, 106682.

Li, P., Hur, J., 2017. Utilization of UV-vis spectroscopy and related data analyses for dissolved organic matter (DOM) studies: a review. Crit. Rev. Environ. Sci. Technol. 47 (3), 131–154.

Li, X., Tsigaris, P., 2024. The global value of freshwater lakes. Ecol. Lett. 27 (2), e14388.

Li, Y., Wang, S., Zhang, L., 2015. Composition, source characteristic and indication of eutrophication of dissolved organic matter in the sediments of Erhai Lake. Environ. Earth Sci. 74, 3739–3751.

Li, Y., Zhang, L., Wang, S., Zhao, H., Zhang, R., 2016. Composition, structural characteristics and indication of water quality of dissolved organic matter in Dongting Lake sediments. Ecol. Eng. 97, 370–380.

Li, S., Fang, J., Zhu, X., Spencer, R.G., Álvarez-Salgado, X.A., Deng, Y., Huang, T., Yang, H., Huang, C., 2022. Properties of sediment dissolved organic matter respond to eutrophication and interact with bacterial communities in a plateau lake. Environ. Pollut. 301, 118996.

Li, W., Li, X., Han, C., Gao, L., Wu, H., Li, M., 2023. A new view into three-dimensional excitation-emission matrix fluorescence spectroscopy for dissolved organic matter. Sci. Total Environ. 855, 158963.

Lin, Y., Hu, E., Sun, C., Li, M., Gao, L., Fan, L., 2023. Using fluorescence index (FI) of dissolved organic matter (DOM) to identify non-point source pollution: the difference in FI between soil extracts and wastewater reveals the principle. Sci. Total Environ. 862, 160848.

Liu, Y., Yang, F., Liu, S., Zhang, X., Li, M., 2023a. Molecular characteristics of microalgal extracellular polymeric substances were different among phyla and correlated with the extracellular persistent free radicals. Sci. Total Environ. 857, 159704.

Liu, S., Hao, Z., Gao, L., Fan, L., Yang, F., Zamyadi, A., Li, M., 2023b. Spatial variation and relationship between soil dissolved organic matter and bacterial community in urban greenspaces. Carbon Res. 2 (1), 13.

Lü, Z.-W., Liu, H.-Y., Wang, C.-L., Chen, X., Huang, Y.-X., Zhang, M.-M., Huang, Q.-L., Zhang, G.-F., 2023. Isolation of endophytic fungi from *Cotoneaster multiflorus* and screening of drought-tolerant fungi and evaluation of their growth-promoting effects. Front. Microbiol. 14, 1267404.

McCrackin, M.L., Jones, H.P., Jones, P.C., Moreno-Mateos, D., 2017. Recovery of lakes and coastal marine ecosystems from eutrophication: a global meta-analysis. Limnol. Oceanogr. 62 (2), 507–518.

Meng, H., Zhang, J., Zheng, Z., Song, Y., Lai, Y., 2024. Classification of inland lake water quality levels based on Sentinel-2 images using convolutional neural networks and spatiotemporal variation and driving factors of algal bloom. Eco. Inform. 80, 102549.

Mielnik, L., Kowalczuk, P., 2018. Optical characteristic of humic acids from lake sediments by excitation-emission matrix fluorescence with PARAFAC model. J. Soils Sediments 18, 2851–2862.

Mostofa, K.M., Li, W., Wu, F., Liu, C.-Q., Liao, H., Zeng, L., Xiao, M., 2018. Environmental characteristics and changes of sediment pore water dissolved organic matter in four Chinese lakes. Environ. Sci. Pollut. Res. 25, 2783–2804.

Nebbioso, A., Piccolo, A., 2013. Molecular characterization of dissolved organic matter (DOM): a critical review. Anal. Bioanal. Chem. 405, 109–124.

Oh, H., Jung, K.-Y., Kim, B.Y., Lee, B.J., Shin, H.-S., Hur, J., 2023. Optimal tracer identification for dissolved organic matter (DOM) source tracking in watersheds using point source effluent load data. Environ. Technol. Innov. 32, 103423.

Pan, B., Liu, S., Ding, Y., Li, M., 2023. Spatial variation and influencing factors of optical characteristic of water extractable organic matter in soils of urban grassland across climatic zones in China. Aquat. Geochem. 29 (4), 189–205.

Pearson, A.R., Fox, B.R., Vandergoes, M.J., Hartland, A., 2022. The sediment fluorescence–trophic level relationship: using water-extractable organic matter to assess past lake water quality in New Zealand. N. Z. J. Mar. Freshw. Res. 56 (2), 213–233.

Qin, B., Paerl, H.W., Brookes, J.D., Liu, J., Jeppesen, E., Zhu, G., Zhang, Y., Xu, H., Shi, K., Deng, J., 2019. Why Lake Taihu continues to be plagued with cyanobacterial blooms through 10 years (2007–2017) efforts. Sci. Bull. 64 (6).

Ren, H., Ma, F., Yao, X., Shao, K., Yang, L., 2020. Multi-spectroscopic investigation on the spatial distribution and copper binding ability of sediment dissolved organic matter in Nansi Lake, China. J. Hydrol. 591, 125289.

Santín, C., Yamashita, Y., Otero, X.L., Álvarez, M.Á., Jaffé, R., 2009. Characterizing humic substances from estuarine soils and sediments by excitation-emission matrix spectroscopy and parallel factor analysis. Biogeochemistry 96 (1), 131–147.

Song, F., Wu, F., Feng, W., Liu, S., He, J., Li, T., Zhang, J., Wu, A., Amarasiriwardena, D., Xing, B., 2019. Depth-dependent variations of dissolved organic matter composition and humification in a plateau lake using fluorescence spectroscopy. Chemosphere 225, 507–516.

Stedmon, C.A., Bro, R., 2008. Characterizing dissolved organic matter fluorescence with parallel factor analysis: a tutorial. Limnol. Oceanogr. Methods 6 (11), 572–579.

Wang, W., Wang, S., Jiang, X., Zheng, B., Zhao, L., Zhang, B., Chen, J., 2018. Differences in fluorescence characteristics and bioavailability of water-soluble organic matter (WSOM) in sediments and suspended solids in Lihu Lake, China. Environ. Sci. Pollut. Res. 25, 12648–12662.

Wen, L., Yang, F., Li, X., Liu, S., Lin, Y., Hu, E., Gao, L., Li, M., 2023. Composition of dissolved organic matter (DOM) in wastewater treatment plants influent affects the efficiency of carbon and nitrogen removal. Sci. Total Environ. 857, 159541.

Xiao, M., Li, M., Duan, P., Qu, Z., Wu, H., 2019. Insights into the relationship between colony formation and extracellular polymeric substances (EPS) composition of the cyanobacterium Microcystis spp. Harmful Algae 83, 34–41.

Xu, Y., Li, P., Zhang, C., Wang, P., 2021. Spectral characteristics of dissolved organic matter in sediment pore water from Pearl River estuary. Sci. China Earth Sci. 64, 52–61.

Yamashita, Y., Jaffé, R., Maie, N., Tanoue, E., 2008. Assessing the dynamics of dissolved organic matter (DOM) in coastal environments by excitation emission matrix fluorescence and parallel factor analysis (EEM-PARAFAC). Limnol. Oceanogr. 53 (5), 1900–1908.

Yang, Z., Zhang, M., Shi, X., Kong, F., Ma, R., Yu, Y., 2016. Nutrient reduction magnifies the impact of extreme weather on cyanobacterial bloom formation in large shallow Lake Taihu (China). Water Res. 103, 302–310.

Yuan, D.-H., Guo, N., Guo, X.-J., Zhu, N.-M., Chen, L., He, L.-S., 2014. The spectral characteristics of dissolved organic matter from sediments in Lake Baiyangdian, North China. J. Great Lakes Res. 40 (3), 684–691.

Zhang, Y., Su, Y., Liu, Z., Yu, J., Jin, M., 2017. Lipid biomarker evidence for determining the origin and distribution of organic matter in surface sediments of Lake Taihu, Eastern China. Ecol. Indic. 77, 397–408.

Zhang, Y., Su, Y., Liu, Z., Sun, K., Kong, L., Yu, J., Jin, M., 2018. Sedimentary lipid biomarker record of human-induced environmental change during the past century in Lake Changdang, Lake Taihu basin, Eastern China. Sci. Total Environ. 613-614, 907–918.

Zhang, Y., Wang, X., Wang, X., Li, M., 2019a. Effects of land use on characteristics of water-extracted organic matter in soils of arid and semi-arid regions. Environ. Sci. Pollut. Res. 26 (25), 26052–26059.

Zhang, R., Huang, Q., Yan, T., Yang, J., Zheng, Y., Li, H., Li, M., 2019b. Effects of intercropping mulch on the content and composition of soil dissolved organic matter in apple orchard on the loess plateau. J. Environ. Manag. 250, 109531.

Zhang, Y., Peng, T., Su, Y., Yu, J., Liu, Z., 2021. Spatial heterogeneity in fatty acid abundance and composition across surface sediments of Lake Taihu, eastern China:

implications for the use of lipids in evaluating carbon cycling and burial in lake systems. CATENA 201, 105225.
Zhou, L., Zhou, Y., Tang, X., Zhang, Y., Jang, K.-S., Székely, A.J., Jeppesen, E., 2021. Resource aromaticity affects bacterial community successions in response to different sources of dissolved organic matter. Water Res. 190, 116776.
Zhou, J., Leavitt, P.R., Zhang, Y., Qin, B., 2022. Anthropogenic eutrophication of shallow lakes: is it occasional? Water Res. 221, 118728.
Zhu, W., Li, M., Luo, Y., Dai, X., Guo, L., Xiao, M., Huang, J., Tan, X., 2014. Vertical distribution of Microcystis colony size in Lake Taihu: its role in algal blooms. J. Great Lakes Res. 40 (4), 949–955.
Zhu, T., Duan, P., He, J., Zhao, M., Li, M., 2017. Sources, composition, and spectroscopiccharacteristics of dissolved organic matter extractedfrom sediments in an anthropogenic-impacted riverin southeastern China. Environ. Sci. Pollut. Res. 24, 25431–25440.
Zhuang, W.-E., Chen, W., Cheng, Q., Yang, L., 2021. Assessing the priming effect of dissolved organic matter from typical sources using fluorescence EEMs-PARAFAC. Chemosphere 264, 128600.
Zsolnay, Á., 2003. Dissolved organic matter: artefacts, definitions, and functions. Geoderma 113 (3–4), 187–209.